Mechanical loss reduction at low temperature after crystallization in a titania-tantala film

Peter G. Murray,[1,*] Jessica Steinlechner,[1,2,3] Hafizah Noor Isa,[4] Rebecca B. Cummings,[1] Raymond Robie,[1] Kieran Craig,[1] Matthew R. Abernathy,[1] Riccardo Bassiri,[5] Martin M. Fejer,[5] James Hough,[1] Ian MacLaren,[1] Sheila Rowan,[1] and Iain W. Martin[1]

[1] *SUPA, School of Physics and Astronomy, University of Glasgow, Glasgow, G12 8QQ, Scotland*
[2] *Maastricht University, P.O. Box 616, 6200 MD Maastricht, The Netherlands*
[3] *Nikhef, Science Park 105, 1098 XG Amsterdam, The Netherlands*
[4] *Department of Physics, Kulliyah of Science, International Islamic University of Malaysia, 25200 Kuantan, Pahang, Malaysia*
[5] *E.L. Ginzton Laboratory, Stanford University, Stanford, California 94305, USA*

(Received 14 June 2024; accepted 17 January 2025; published 11 February 2025)

Due to its excellent optical properties, such as low absorption and scattering, amorphous Ta_2O_5 is commonly used as an optical coating material, often in combination with SiO_2 layers to produce a highly reflective stack. However, the high mechanical loss of Ta_2O_5 limits the thermal-noise performance of such coatings when used in precision measurement applications. Doping with TiO_2 has previously been shown to slightly reduce the mechanical loss, but it is still very high compared to many other materials, particularly at low temperatures. In this paper, we present a detailed study of different heat treatment temperatures and of Ti concentrations of up to nominally 75%. We show a significant mechanical-loss reduction for the mixture with the highest Ti cation content, which crystallized after heat treatment at 500°C. The resulting loss is much lower than that of pure TiO_2 or that of Ta_2O_5 after crystallization, making further studies highly interesting, in particular investigations of scattering which may pose a major drawback for optical applications.

DOI: 10.1103/PhysRevD.111.042005

I. INTRODUCTION

Tantalum pentoxide (Ta_2O_5), in its amorphous state, is widely used as a material for optical coatings [1,2]. Such coatings are made of stacks of thin films of two alternating materials, different in refractive index. Ta_2O_5 is commonly used as the high-index material in combination with silica (SiO_2) as the low-index material. The index contrast leads to reflection at the layer interfaces so that, by accurately tuning the layer thicknesses, coatings of various reflectivities can be created such as highly reflective coatings, antireflection coatings or coatings with a certain splitting ratio.

When deposited via ion-beam sputtering, highly reflective mirror coatings made of SiO_2 and Ta_2O_5 show excellent optical properties such as extremely low optical absorption and scattering [3]. These coatings form the basis of a variety of high-precision experiments in quantum optics and related fields, involving high laser power or low optical losses [4]. The fields of gravitational-wave detection and laser stabilization, e.g., for atomic-clock development [2], share an additional requirement: low thermal noise of the highly reflective coated mirrors.

Coating thermal noise is proportional to the mechanical loss of the coating [5], which is related to the individual losses of the contributing materials. The mechanical loss of Ta_2O_5 is considerably higher than that of SiO_2 [6]. Studies show that titania (TiO_2) doping can reduce the mechanical loss of Ta_2O_5 significantly [7–10]. Despite extensive effort for more than a decade, involving different doping materials and elevated temperature deposition based on structural modeling results, no further significant mechanical-loss reduction in Ta_2O_5 has been possible to date—when using the material at room temperature.

An option to reduce coating thermal noise is cooling of the mirrors to cryogenic temperatures. However, the mechanical loss of Ta_2O_5 has been shown to increase toward low temperatures with a peak at around 20 K, at which the mechanical loss is about a factor of 5 higher than at room temperature [11,12]. Consequently, the thermal-noise reduction from a temperature decrease is partly compensated by this loss increase. Doping with

[*] Contact author: peter.murray@glasgow.ac.uk

TABLE I. Ti cation percentages as proportion of all metals (Ti + Ta) in the $TiO_2 - Ta_2O_5$ films. In the text we refer to the nominal concentrations, specified by CSIRO, while measurements using electron energy loss spectroscopy found lower Ti concentrations, different for measurements A and B—see main text for details. Measurement B was carried out on samples heat treated at different temperatures.

		Measured	
Ti concentrations	Nominal (%)	A	B
Low	25	$(14 \pm 3)\%$ [19]	$(11.2 \pm 0.1)\%$ (200°C) [20]
Low			$(8.5 \pm 1.2)\%$ (400°C) [20]
Low			$(10.4 \pm 0.5)\%$ (600°C) [20]
Medium	55	$(52 \pm 10)\%$ [19]	$(43.9 \pm 2.3)\%$ (600°C) [20]
High	75	$(68 \pm 1)\%$ [19]	...

14.5% Ti slightly reduces the magnitude of the peak, but increases its width [12]. In the same reference, it has been observed that the distribution of potential barriers in the material shows a shift toward higher energies with TiO_2 doping. Higher doping concentrations may result in a further shift and a consequent thermal-noise reduction, as has been suggested by molecular dynamics modeling results showing decreasing cryogenic loss with increasing doping [13]. This makes more detailed research into the low-temperature mechanical loss, revealing information about the barrier distribution, of Ta_2O_5 doped with different concentrations of Ti of interest.

Postdeposition heat treatment is commonly used to reduce the optical absorption and the mechanical loss of optical coatings. For (TiO_2 doped) Ta_2O_5 coatings, used at room temperature, an optimum heat-treatment temperature of around 500–600°C has been identified. At low temperatures, the peak mechanical loss is about a factor of 2 lower after heat treatment at 300–400°C than after 600°C, originally investigated by Martin *et al.* [14], and occurs at a higher temperature of around 40 K. Molina-Ruiz *et al.* [15] also observed a low temperature loss peak around 50 K from measurements of double paddle oscillators coated with magnetron sputtered tantala films after 500°C and 600°C anneals. X-ray diffraction measurements by Vajente *et al.* [16] of IBS tantala coatings have shown they remain amorphous after anneals up to 500°C. Above 600°C, the Ta_2O_5 crystallizes and a high, broad low-temperature mechanical-loss peak develops [14]. However, TiO_2 is known to crystallize at much lower temperatures of around 300°C [17] so that an increase in Ti doping concentration may also change the optimum heat-treatment temperature of the Ta_2O_5.

In this paper, we present low-temperature mechanical-loss measurements of Ta_2O_5 with three different concentrations of Ti (see Table I for detail), at different heat-treatment temperatures. We show that for the two lower Ti concentrations, of nominally 25 and 55%, the temperature-dependent mechanical loss resembles that of pure Ta_2O_5. However, for a nominal concentration of 75% Ti, the mechanical loss drops drastically, in particular at low temperatures, after heat treatment at 500°C, likely due to crystallization of the coating [18]. While also showing a reduction in mechanical loss when crystallizing, the resulting loss of pure TiO_2 is significantly higher than that of the TiO_2 and Ta_2O_5 mix.

II. DEPOSITION OF THE FILMS MEASUREMENT OF THE DIFFERENT TI CONCENTRATIONS

Silicon cantilevers [21] were coated by ion-beam sputtering by CSIRO.[1] The design thickness of the layers was $t_{\mathrm{coat}} = (500 \pm 10)$ nm. The Ti cation concentrations were nominally 25%, 55%, and 75%. The actual stoichiometry was determined via electron energy loss spectroscopy (EELS) measurements and initially found to be 14%, 52%, and 68% [19], see measurement A in Table I.

The initial concentration measurements were then reviewed using a more quantitative approach. This was based on determination of absolute cross-sections for the excitation of specific absorption edges, in a manner analogous to that previously used by Craven *et al.* [22], and the subsequent use of these by fitting the spectrum as a linear combination of the standards by Craven *et al.* [23]. In this case, standards were developed for the $N_{4,5}$ edge of Ta at about 229 eV, for which no calculated cross-section exists, and the $L_{2,3}$ edge of Ti at around 456 eV. No attempt was made to measure the O content and it was assumed, since the oxygen concentration would not affect the measurements on the titanium to tantalum ratio, that there were 2.5 oxygens per Ta atom and 2 per Ti atom. Since performing this work, it has become apparent that there is a small amount of Ar incorporated in the films in nanosized bubbles, and amounting to maybe 1–3% of the atoms in there [10,24,25]. This would modify the Ta edge shape slightly, as the $L_{2,3}$ sits a little after the 229 eV onset of the Ta at 245 eV. However, this did not affect fits significantly as first, the Ar content is small in the film as a whole and second, both the Ta_2O_5 film standard and the films being quantified contained similar argon contents as far as we can

[1] Commonwealth Scientific and Industrial Research Organization, Australia.

tell. Fitting these gave excellent results and low residuals. More information and exact technical details are given in the thesis by Isa [20]. Full details of the results for measurement B are given in Table I.

While the measurements of the highest Ti concentration were not repeated, Isa reports a Ti concentration of 43.9% for the nominally 55% Ti doped Ta_2O_5 coating. For the lowest doping concentration, small variations in the Ti content were found for different heat treatment temperatures while the as-deposited coating was not investigated. It is unclear why the doping concentration changes due to heat treatment, but it is likely that there are small variations in Ti concentration across the films to which the analysis method is sensitive as only areas of a few hundred nanometres across were probed, and any small variations on the scale of tens of microns or even millimetres would not be seen. While all measurements (A and B) agree that the actual Ti concentrations are lower than the design percentage, we will refer to the nominal values here for consistency with previous reports [19,20,26–29].

III. MECHANICAL LOSS OF THE AS-DEPOSITED COATINGS FOR DIFFERENT TI CONCENTRATIONS

The mechanical loss of the coated cantilevers, ϕ_{total}, was determined by exciting resonant (bending) modes and measuring the decay of the oscillation. The mechanical loss of the coatings was calculated from the measured total loss via

$$\phi_{\text{coat}} = \frac{Y_{\text{sub}} t_{\text{sub}}}{3 Y_{\text{coat}} t_{\text{coat}}} (\phi_{\text{total}} - \phi_{\text{sub}}), \tag{1}$$

where Y_{sub} and Y_{coat} are the Young's moduli of the cantilever and the coating and ϕ_{sub} is the mechanical loss of the uncoated cantilever.[2] The cantilever thickness, t_{sub}, was calculated for each sample from the frequencies of the resonant modes measured and was between 44 and 70 μm for the silicon cantilevers used in this study. A detailed description of the measurement procedure can be found in [31]. Figure 1(a) shows an example of mechanical losses of an uncoated cantilever (bottom), the measured loss of the coated cantilever (middle) and the coating loss calculated using Eq. (1).

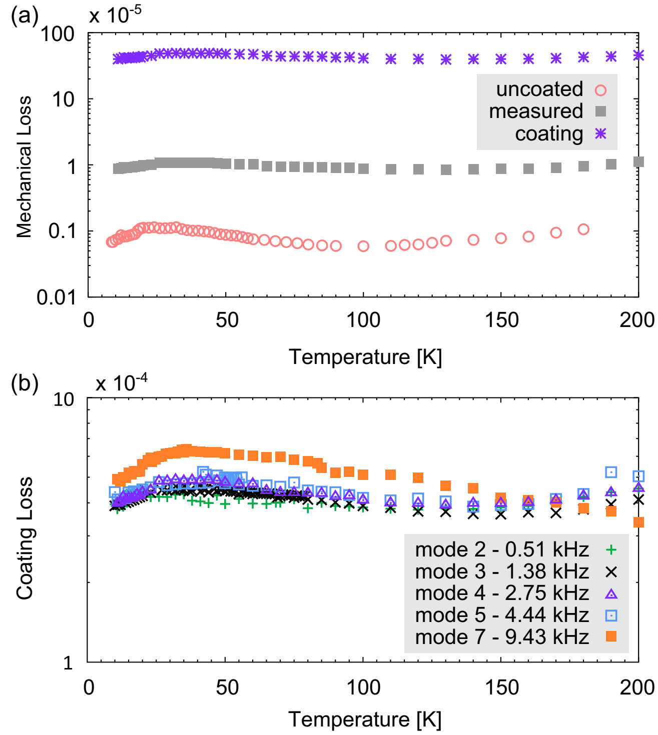

FIG. 1. Mechanical loss as a function of temperature. (a) shows the mechanical loss of a so-called control sample, i.e. an uncoated cantilever (bottom, red circles), the mechanical loss as measured of the coated cantilever (middle, gray squares) and the coating loss calculated using Eq. (1) (top, purple stars). The coating loss is shown for the coating with a nominal TiO_2 concentration of 25% (identical to the purple starts in Fig. 2. (b) shows different modes of the same coating [mode four is identical too that shown in (a) and in Fig. 3, all shown in purple].

The mechanical loss was measured as a function of heat treatment temperature. For each sample, several resonant modes were measured. In this paper, we show results for the fourth bending mode at ≈2500 Hz: in all cases, these are broadly representative of the losses measured for other modes. Figure 2(b) shows an example of the mechanical loss as a function of temperature of four different modes of the same sample.

Figure 2 shows the temperature-dependent mechanical loss of the as-deposited coatings for pure Ta_2O_5 (green) and for Ta_2O_5 with different Ti concentrations: 25% (purple) and 55% (pink) result in a similar loss level, significantly lower than that of pure Ta_2O_5 over the whole temperature range. For 75% Ti (orange), the loss is similar to that of pure TiO_2 (blue)—higher than that of the films with lower Ti concentrations, but lower than of pure Ta_2O_5. This leads

[2]For pure Ta_2O_5 and for the lower Ti concentrations, the Young's moduli (Y) used for the mechanical loss analysis were measured via nanoindentation for all heat treatment steps [26]. For the coatings with a 75% Ti concentration and pure TiO_2, values of $Y_{\text{Ta}} = (151 \pm 4)$ GPa and $Y_{\text{Ti}} = (155 \pm 5)$ GPa were obtained using a linear extrapolation from the films with lower Ti concentrations, which we concluded to be valid due to agreement of the result for pure TiO_2 with literature. However, the Young's modulus of pure TiO_2 is known to change with crystallization [30]. In [30], Anderson *et al.* present measurements of the Young's modulus of pure TiO_2 films with as-deposited values similar to that of our coating, and a similar crystallization temperature. The Young's modulus of their films increased by about 25% after crystallization (from ≈147 GPa to ≈185 GPa). Such a potential change, which was not included in our model, would change our results for the coating mechanical loss by approximately the same amount. Even if this was the case, our overall result of a significant loss reduction of the Ta_2O_5 with 75% Ti concentration would be still valid.

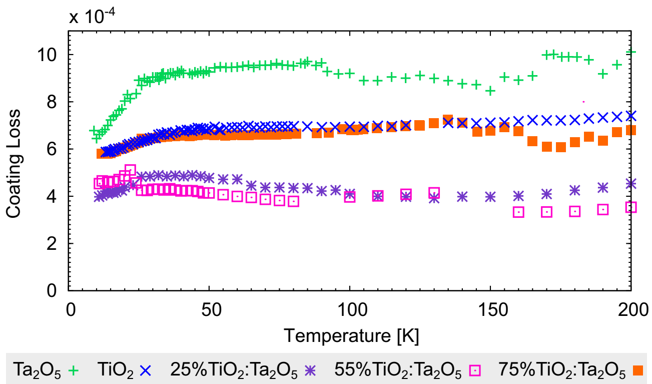

FIG. 2. Mechanical loss as a function of temperature for coatings as deposited. Shown are measurements on Ta_2O_5 films with Ti concentrations (as TiO_2) of nominally 25%, 55%, and 75%. Measurements on pure Ta_2O_5 and TiO_2 are shown for comparison. All graphs in this paper show measurements made on the fourth bending mode to represent the mechanical-loss trends observed.

to the assumption that a Ti concentration between 25% and 55% is ideal for loss reduction. However, we find that heat treatment of the coatings changes this picture.

IV. MECHANICAL LOSS AS A FUNCTION OF HEAT TREATMENT TEMPERATURE

Figure 3(a) shows the temperature-dependent mechanical loss of pure Ta_2O_5 for different heat-treatment temperatures. The green points are identical to those shown in Fig. 2. For heat treatment at 300°C (dark blue) and 400°C (light blue), the loss reduces to a very similar level. After heat treatment at 500°C,[3] the loss increases slightly. At 600°C (red) a peak at around 20 K develops. After heat treatment at 800°C (gray), a broad and high loss peak with a maximum at around 90 K forms, which far exceeds the loss of the as-deposited coating.

Figure 3(b) shows the mechanical loss as a function of temperature for pure TiO_2. The loss of the as-deposited coating (blue, identical to the blue curve in Fig. 2) reduces slightly for heat treatment at 150°C (green). After heat treatment at 300°C (yellow), the loss drops significantly. As TiO_2 is known to crystallize at temperatures below 300°C [17], this coating was not heat treated to any higher temperatures. It is interesting that crystallization reduces the mechanical loss of pure TiO_2, while that of pure Ta_2O_5 increases.

Figure 4(a) shows the Ta_2O_5 coating with a nominal concentration of 25% Ti, heat treated at different temperatures. While heat treatment at 300°C (blue) slightly

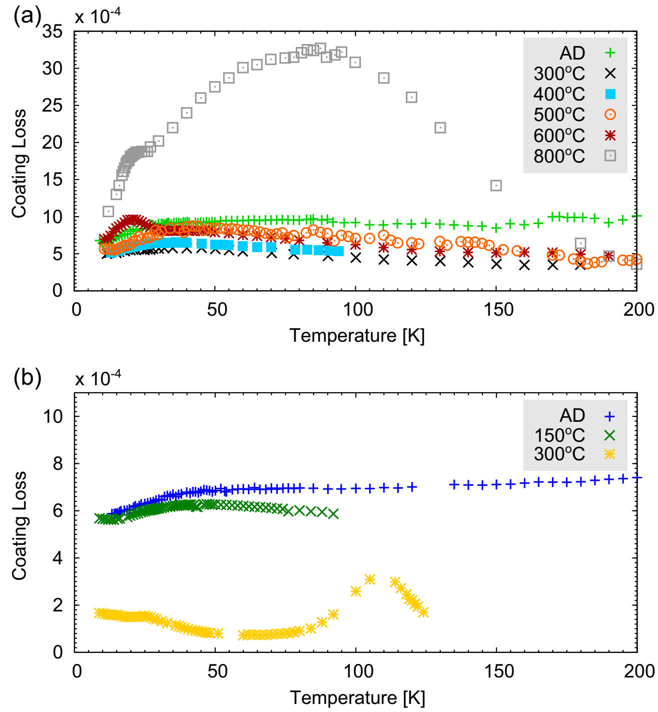

FIG. 3. Mechanical loss as a function of temperature, for samples heat treated at different temperatures: (a) pure Ta_2O_5, (heat treated data previously published in [14]) and (b) pure TiO_2.

reduces the mechanical loss compared to the as deposited coating (purple, identical to the purple curve in Fig. 2), for heat treatment at higher temperatures, a loss peak at around 30 K starts to form (yellow and green).

Measurements on the coating with a nominal concentration of 55% Ti—an almost equal mix of the two materials—show the development of a similar peak than observed for the lowest Ti concentration after heat treatment at 600°C (brown), see Fig. 4(b). This is also very similar to the peak shown by pure Ta_2O_5 and by Ta_2O_5 with 14.5% Ti concentration, previously studied [11].

For the highest Ti concentration of 75%, we get a very different picture as shown in Fig. 4(c). After heat-treatment at 500°C (dark blue), the mechanical loss decreases drastically. Heat treatment at 600°C does not change the loss much at most temperatures, but below 25 K a further reduction can be observed (light blue). A second sample, heat treated at 600°C (black) confirmed the low mechanical-loss level of the Ta_2O_5 coating with 75% Ti concentration.

Figure 5 shows a direct comparison of the Ta_2O_5 films with different Ti concentrations, after heat treatment at 600°C. For pure Ta_2O_5 and for the lower Ti concentrations, the magnitude of the mechanical loss is similar at low temperatures, with a peak at around 20 K. Although starting at a much higher loss level, as-deposited (see Fig. 2), the coating with 75% Ti concentration shows a mechanical loss more than an order of magnitude lower around 20 K after

[3]While all the other coatings pure Ta_2O_5 were produced in the same coating run, the coating heat treated at 500°C came from a different coating run, produced by the same vendor and same deposition method.

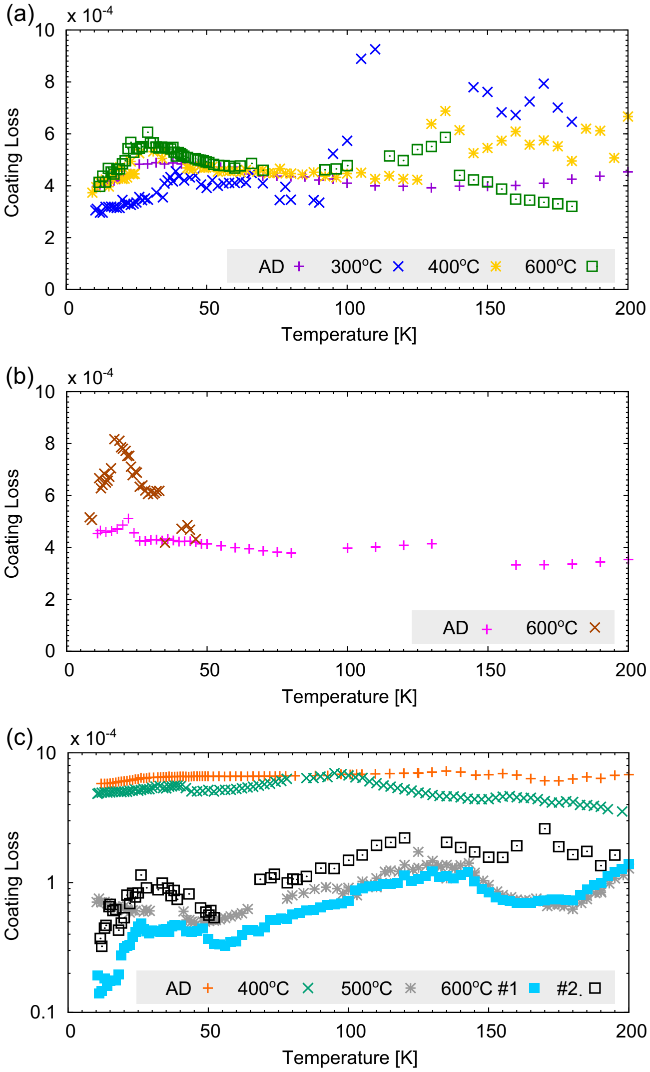

FIG. 4. Temperature-dependent mechanical loss for different heat-treatment steps of Ta_2O_5 films with (a) 25% Ti concentration, (b) 55% Ti concentration, and (c) 75% Ti concentration.

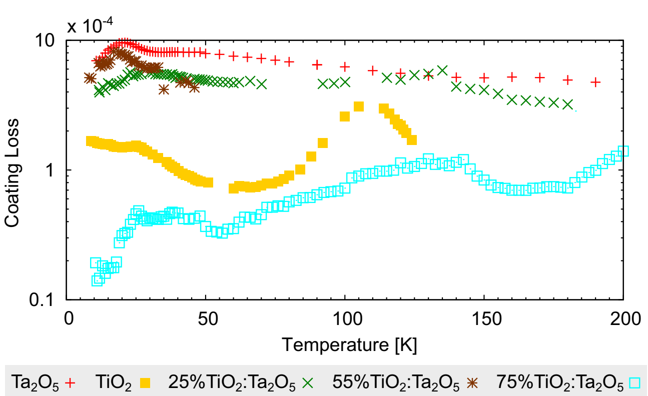

FIG. 5. Temperature-dependent mechanical loss after heat treatment of pure Ta_2O_5, pure TiO_2 and of Ta_2O_5 with different Ti concentrations. All coatings were heat-treated at 600°C, except the pure TiO_2 coating which was not further heat treated after crystallizing at 300°C.

heat treatment (light blue). Remarkably, this loss level is also significantly lower than that of pure TiO_2 after crystallization (yellow—this coating was not further heat treated after crystallizing at 300°C), in particular at temperatures of around 20 K and below.

V. ANALYSIS OF THE FILM STRUCTURE

The structure of the Ta_2O_5 film with a nominal Ti concentration of 75% has been investigated using a witness sample with the film deposited on an SiO_2 substrate. Ta_2O_5 remains amorphous for heat treatment at 600°C [14], while Ta_2O_5 with a nominal Ti concentration of 75% has previously been shown to adopt a polycrystalline structure for heat treatment at the same temperature [18]. This is examined in more detail in Fig. 6, which shows results from scanning precession electron diffraction carried out in the transmission electron microscope [32] resulting in a 4D dataset (2 spatial dimensions and 2 k-space dimensions), all carried out on a cross-section through the film and substrate surface made using a conventional focused ion beam liftout method) [33,34]. The scans were performed on a JEOL ARM200F using an accelerating voltage of 200 kV, the smallest available spotsize (5) and the smallest condenser aperture (10 μm) resulting in a small spot of ∼2 nm in size and clear separation of all discrete diffraction spots in the resulting diffraction patterns.

Figure 6(a) shows an annular dark field (ADF) image [35] calculated from the 4D dataset (using the py4DSTEM package [36]). As would be expected for ADF, the film, containing heavier elements like Ta and Ti, is brighter than the SiO_2 in the substrate (but does not have uniform thickness, resulting in some grayscale contrast variations). Nevertheless, the Pt-C coating (used to protect the surface in Focused Ion Beam liftout) above the film is also bright at the top of the film (with a very thin dark C-rich layer between the two, which is not unusual in Pt-C deposition).

The film was found to have crystallized into the anatase structure (a common polymorph of TiO_2), both by thin film grazing incidence x-ray diffraction, and by electron diffraction. Figure 6(b) is a crystal orientation map made using the ACOM (automated crystal orientation mapping) module of py4DSTEM [36,37] and represented using the ORIX library [38] for the anatase-TiO_2 structure. Representative diffraction patterns of the two grains (averaged from the orange and purple boxes in Fig. 6(a) are shown in Figs. 6(c) and 6(d). For reference, a diffraction pattern from amorphous SiO_2 image averaged from the mid-blue box on Fig. 6(a) is shown in Fig. 6(e). This demonstrates not that only is the film crystallized, but that the crystals have grown really rather large in 24 h, with lateral extents of well over 1 μm—likely a better measure of size would be possibly with electron backscatter diffraction (EBSD). As the significant change in mechanical loss already occurs after heat treatment at 500°C, see Fig. 4(c), it is likely that the film had already started to crystallize at that temperature,

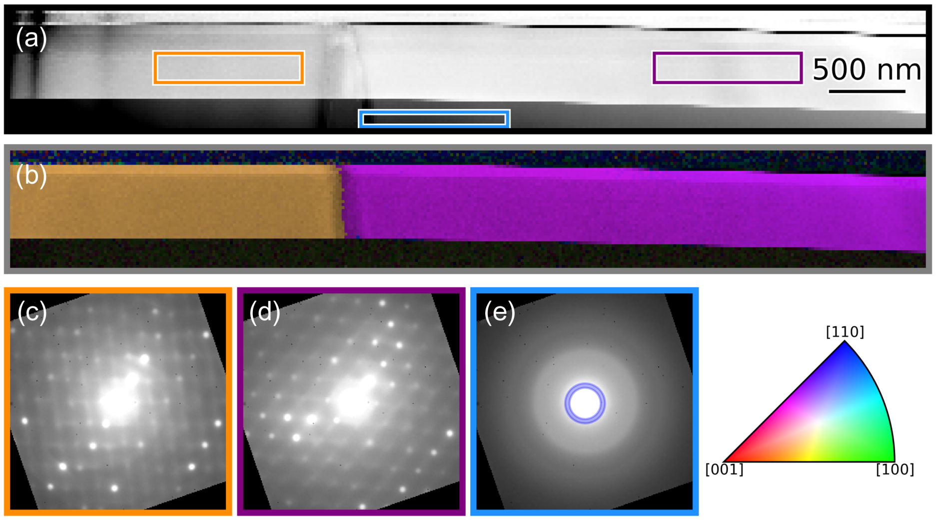

FIG. 6. Scanning precession electron diffraction characterization of a Ta_2O_5 film with a nominal Ti concentration of 75% heat treated at 600°C: (a) annular dark field image calculated from the 4D dataset; (b) orientation map for anatase where the color represents the crystal direction in the direction out-of-the-page according to the key shown in the bottom right; (c),(d) representative diffraction patterns for grains 1 and 2 (from the orange and purple boxes in (a); and (e) representative diffraction pattern for the amorphous SiO_2.

even if significant crystal growth only happened at rather higher temperatures.

This is radically different to TiO_2:Ta_2O_5 films with lower contents after heat treatment. Samples with about 50%–55% Ti remain amorphous even after 600°C heat treatment [39] and the main features of the short range order of those samples are still mainly similar to those for Ta_2O_5 and for TiO_2:Ta_2O_5 with lower Ti contents, even if a shoulder starts to appear on the second nearest neighbor peaks from Ti-Ta neighbors [39]. In contrast to this, at the high Ti contents studied in the present paper, a radical structure transformation has occurred with an atomic ordering much more characteristic of TiO_2 than Ta_2O_5, and this crystallizes far more readily on heat treatment.

VI. DISCUSSION OF THE LOSS REDUCTION

Favaro *et al.* [40] reported the reduction of the mechanical loss in ion-beam sputtered Ta_2O_5 thin films through partial crystallization at room temperature. It is therefore interesting that the cryogenic mechanical loss of pure TiO_2 is also observed here to reduce with crystallization, see Fig. 3(b), while, at low temperatures, that of pure Ta_2O_5 increases, see Fig. 3(a). Lalande *et al.* [41] showed that, at room temperature, the mechanical loss of coatings comprising of a zirconia-titania-tantala ternary alloy, with a low-to-medium zirconia and titania doping, increased after crystallization. However, the higher doped samples were not only able to withstand annealing temperatures of over 800°C without crystallizing, the room temperature Brownian thermal noise of these coatings were up to 20% lower than the current Advanced LIGO coatings. This suggests that the study of the cryogenic mechanical loss of ternary coatings, heat treated near their crystallization point, could be of future interest. That the Ta_2O_5 with a nominal Ti concentration of 75% crystallizes at a higher temperature than the pure TiO_2 is not unexpected. However, it is highly interesting that the mechanical loss after crystallization reduces to a level significantly below that of crystallized pure TiO_2, as Diksha *et al.* [42] also observed the absorption of a near-pure TiO_2 film to reduce after crystallization, which is a property which for other materials has been shown to worsen after crystallization [43].

The origin of the reduced mechanical loss is unknown. Many crystalline materials show excellent optical and mechanical properties and are very interesting for a variety of optical applications. However, usually only single-crystalline materials such as silicon or sapphire for (bulk) substrates [44,45] or single-crystalline coatings such as AlGaAs or GaP are considered [46–53] for application in precision optics, as materials forming polycrystalline structures from heat treatment commonly show an increase in mechanical loss, in optical absorption and, in particular, in optical scattering.

It does seem that a large-grained (if not monocrystalline) structure developed in the films investigated here. A possible explanation for the low mechanical loss is that the large size of the crystals means that boundaries represent a miniscule volume fraction and consequently hardly contribute to the mechanical loss over the measured temperature range. Another option previously suggested is that individual crystals could be surrounded by thin amorphous regions, reducing the contribution of the mechanical loss from the amorphous material and allowing the coating to behave more like a single crystal [54,55], but there was no evidence of amorphous boundaries seen to date.

VII. SUMMARY

We have shown a significant decrease in low-temperature mechanical loss of Ta_2O_5 with a nominal Ti cation concentration of 75% (see Table I for details of the nominal vs measured concentration), when heat treated above crystallization temperature. This reduction is in contrast to pure Ta_2O_5 which shows a significant increase in mechanical loss when forming a polycrystalline structure due to heat treatment. While the mechanical loss of pure TiO_2 also decreases when crystallizing, the resulting mechanical loss is an order of magnitude higher at 10–20 K than that of the mix. Possible explanations are a different grain size of the crystallized regions or a separation of the grains by amorphous regions. The results presented here suggest that the mechanical loss reduces when the coating changes from amorphous to partially crystalline. Therefore, in order to further understand the relationship between mechanical loss and crystallization, further studies of high-quality titania-doped tantala coatings are of significant interest, particularly beyond the crystallization point.

While a polycrystalline structure may cause a level of scattering which is problematic for applications in precision optics, it is interesting to note that titania-silica mixed films, while showing an increase in scatter on crystallization, are still compatible with the scattering requirements of gravitational wave detectors [56]. Pure TiO_2 films have shown a continuing decrease in absorption with heat treatment beyond crystallization [57]. The major reduction in mechanical loss observed after crystallization would result in a significant improvement in thermal noise compared to e.g. Ta_2O_5 with no or low Ti doping. Therefore, the unexpected reduction in low-temperature mechanical loss of the Ta_2O_5 coating with a nominal Ti concentration of 75% provides a strong motivation for further investigation of other material properties such as optical absorption and scattering.

ACKNOWLEDGMENTS

We are grateful for financial support from STFC (Grants No. ST/L000946/1, No. ST/N005422/1, No. ST/V005634/1), the Royal Society (RG110331) and the University of Glasgow. I. W. M. was supported by a Royal Society Research Fellowship while working on this paper. We are thankful for funding of the Ph.D. of Hafizah Noor Isa by the Islamic International University of Malaysia (IIUM) and Ministry of Higher Education (MoHE) Malaysia. R. B. C. is grateful to the Engineering and Physical Sciences Research Council for funding a PhD studentship (No. EP/R513222/1). R. B. and M. M. F. acknowledge the support of the LSC Center for Coatings Research, jointly funded by the National Science Foundation (NSF) and the Gordon and Betty Moore Foundation (GBMF). In particular, the authors are grateful for support through NSF Awards No. PHY-1707866, No. PHY-1708175 and GBMF Grant No. 6793. J. S. acknowledges support by ETpathfinder (Interreg Vlaanderen-Nederland), E-TEST (Interreg Euregio Meuse-Rhine), the Dutch Research Council (NWO) Project No. VI.Vidi.203.062, and the Province of Limburg. We are grateful to the International Max Planck Partnership for Measurement and Observation at the Quantum Limit for support, and we thank our colleagues in the LSC and Virgo collaborations and within SUPA for their interest in this work. This paper has LIGO Document number LIGO-P2400213.

DATA AVAILABILITY

The data presented in this paper can be accessed at [58].

[1] M. Granata, A. Amato, L. Balzarini, M. Canepa, J. Degallaix, D. Forest, V. Dolique, L. Mereni, C. Michel, L. Pinard, B. Sassolas, J. Teillon, and G. Cagnoli, Amorphous optical coatings of present gravitational-wave interferometers, Classical Quantum Gravity **37**, 095004 (2020).

[2] D. G. Matei, T. Legero, S. Häfner, C. Grebing, R. Weyrich, W. Zhang, L. Sonderhouse, J. M. Robinson, J. Ye, F. Riehle, and U. Sterr, 1.5 μm lasers with sub-10 mHz linewidth, Phys. Rev. Lett. **118**, 263202 (2017).

[3] L. Pinard, C. Michel, B. Sassolas, L. Balzarini, J. Degallaix, V. Dolique, R. Flaminio, D. Forest, M. Granata, B. Lagrange, N. Straniero, J. Teillon, and G. Cagnoli, Mirrors used in the LIGO interferometers for first detection of gravitational waves, Appl. Opt. **56**, C11 (2017).

[4] Y. Pu, P. Ma, Z. Qiao, M. Zhang, Z. Lu, F. Qiu, and L. Lv, Annealing effects on microstructure and laser-induced damage threshold of quasi-rugate filters, Opt. Express **24**, 23044 (2016).

[5] G. M. Harry, A. M. Gretarsson, P. R. Saulson, S. E. Kittelberger, S. D. Penn, W. J. Startin, S. Rowan, M. M. Fejer, D. R. M. Crooks, G. Cagnoli, J. Hough, and N. Nakagawa, Thermal noise in interferometric gravitational wave detectors due to dielectric optical coatings, Classical Quantum Gravity **19**, 897 (2002).

[6] D. R. M. Crooks, G. Cagnoli, M. M. Fejer, A. Gretarsson, G. Harry, J. Hough, N. Nakagawa, S. Penn, R. Route, S. Rowan, and P. H. Sneddon, Experimental measurements of coating mechanical loss factors, Classical Quantum Gravity **21**, S1059 (2004).

[7] G. M. Harry *et al.*, Titania-doped tantala/silica coatings for gravitational-wave detection, Classical Quantum Gravity **24**, 405 (2006).

[8] R. Flaminio, J. Franc, C. Michel, N. Morgado, L. Pinard, and B. Sassolas, A study of coating mechanical and optical losses in view of reducing mirror thermal noise in gravitational wave detectors, Classical Quantum Gravity **27**, 084030 (2010).

[9] A. Amato, G. Cagnoli, M. Canepa, E. Coillet, J. Degallaix, V. Dolique, D. Forest, M. Granata, V. Martinez, C. Michel, L. Pinard, B. Sassolas, and J. Teillon, High-reflection coatings for gravitational-wave detectors: State of the art and future developments, J. Phys. Conf. Ser. **957**, 012006 (2018).

[10] M. A. Fazio, G. Vajente, A. Ananyeva, A. Markosyan, R. Bassiri, M. M. Fejer, and C. S. Menoni, Structure and morphology of low mechanical loss TiO_2-doped Ta_2O_5, Opt. Mater. Express **10**, 1687 (2020).

[11] I. Martin, H. Armandula, C. Comtet, M. M. Fejer, A. Gretarsson, G. Harry, J. Hough, J.-M. M. Mackowski, I. MacLaren, C. Michel, J.-L. Montorio, N. Morgado, R. Nawrodt, S. Penn, S. Reid, A. Remillieux, R. Route, S. Rowan, C. Schwarz, P. Seidel, W. Vodel, and A. Zimmer, Measurements of a low-temperature mechanical dissipation peak in a single layer of Ta_2O_5 doped with TiO_2, Classical Quantum Gravity **25**, 055005 (2008).

[12] I. W. Martin *et al.*, Comparison of the temperature dependence of the mechanical dissipation in thin films of Ta_2O_5 and Ta_2O_5 doped with TiO_2, Classical Quantum Gravity **26**, 155012 (2009).

[13] J. P. Trinastic, R. Hamdan, C. Billman, and H.-P. Cheng, Molecular dynamics modeling of mechanical loss in amorphous tantala and titania-doped tantala, Phys. Rev. B **93**, 014105 (2016).

[14] I. W. Martin, R. Bassiri, R. Nawrodt, M. M. Fejer, A. Gretarsson, E. Gustafson, G. Harry, J. Hough, I. MacLaren, S. Penn, S. Reid, R. Route, S. Rowan, C. Schwarz, P. Seidel, J. Scott, and A. L. Woodcraft, Effect of heat treatment on mechanical dissipation in Ta_2O_5 coatings, Classical Quantum Gravity **27**, 225020 (2010).

[15] M. Molina-Ruiz, K. Shukla, A. Ananyeva, G. Vajente, M. R. Abernathy, T. H. Metcalf, X. Liu, A. Markosyan, R. Bassiri, M. M. Fejer, M. Fazio, L. Yang, C. S. Menoni, and F. Hellman, Low mechanical loss and high refractive index in amorphous Ta_2O_5 films grown by magnetron sputtering, Phys. Rev. Mater. **8**, 035603 (2024).

[16] G. Vajente *et al.*, Effect of elevated substrate temperature deposition on the mechanical losses in tantala thin film coatings, Classical Quantum Gravity **35**, 075001 (2018).

[17] H.-W. Pan, S.-J. Wang, L.-C. Kuo, S. Chao, M. Principe, I. M. Pinto, and R. DeSalvo, Thickness-dependent crystallization on thermal anneal for titania/silica nm-layer composites deposited by ion beam sputter method, Opt. Express **22**, 29847 (2014).

[18] I. Martin, K. Craig, P. Murray, R. Robie, S. Reid, A. Cumming, R. Bassiri, M. M. Fejer, J. Harris, M. Hart, G. Harry, K. Haughian, D. Heinert, J. Hough, A. Lin, I. MacLaren, R.Nawrodt, S. Penn, R. Route, and S. Rowan, Presentation at GWADW: Mechanical loss of crystalline and amorphous coatings (2014), https://www.gravity.phys.titech.ac.jp/GWADW2014/slide/Iain_Martin.pdf.

[19] R. Bassiri, M. R. Abernathy, F. Liou, A. Mehta, E. K. Gustafson, M. J. Hart, H. N. Isa, N. Kim, A. C. Lin, I. MacLaren, I. W. Martin, R. K. Route, S. Rowan, B. Shyam, J. F. Stebbins, and M. M. Fejer, Order, disorder and mixing: The atomic structure of amorphous mixtures of titania and tantala, J. Non-Cryst. Solids **438**, 59 (2016).

[20] H. N. Isa, Towards reliable quantification of mixed oxide coating for LIGO using DualEELS, Ph.D. thesis, University of Glasgow, 2019, http://theses.gla.ac.uk/74354.

[21] P. G. Murray, I. W. Martin, K. Craig, J. Hough, R. Robie, S. Rowan, M. R. Abernathy, T. Pershing, and S. Penn, Ion-beam sputtered amorphous silicon films for cryogenic precision measurement systems, Phys. Rev. D **92**, 062001 (2015).

[22] A. J. Craven, J. Bobynko, B. Sala, and I. MacLaren, Accurate measurement of absolute experimental inelastic mean free paths and EELS differential cross-sections, Ultramicroscopy **170**, 113 (2016).

[23] A. J. Craven, B. Sala, J. Bobynko, and I. MacLaren, Spectrum imaging of complex nanostructures using DualEELS: II. absolute quantification using standards, Ultramicroscopy **186**, 66 (2018).

[24] R. B. Cummings, R. Bassiri, I. W. Martin, and I. MacLaren, Argon bubble formation in tantalum oxide-based films for gravitational wave interferometer mirrors, Opt. Mater. Express **11**, 707 (2021).

[25] R. B. Cummings, Using electron energy loss spectroscopy to investigate the structure of the mirror coatings of gravitational wave detectors, Ph.D. thesis, University of Glasgow, 2023, https://theses.gla.ac.uk/83489/.

[26] M. R. Abernathy, Mechanical properties of coating materials for use in the mirrors of interferometric gravitational wave detectors, Ph.D. thesis, University of Glasgow, 2012, http://theses.gla.ac.uk/3671.

[27] K. Craig, Studies of the mechanical dissipation of thin films for mirrors in interferometric gravitational wave detectors, Ph.D. thesis, University of Glasgow, 2015, http://theses.gla.ac.uk/6582.

[28] M. J. Hart, Amorphous mirror coatings for ultra-high precision interferometry, Ph.D. thesis, University of Glasgow, 2017, http://theses.gla.ac.uk/8407.

[29] R. Robie, Characterisation of the mechanical properties of thin-film mirror coating materials for use in future interferometric gravitational wave detectors, Ph.D. thesis, University of Glasgow, 2018, http://theses.gla.ac.uk/30645.

[30] O. Anderson, C. Ottermann, R. Kuschnereit, P. Hess, and K. Bange, Density and Young's modulus of thin TiO_2 films, Fresenius J. Anal. Chem. **358**, 315 (1997).

[31] S. Reid, G. Cagnoli, D. R. M. Crooks, J. Hough, P. Murray, S. Rowan, M.M. Fejer, R. Route, and S. Zappe, Mechanical dissipation in silicon flexures, Phys. Lett. A **351**, 205 (2006).

[32] E. F. Rauch, J. Portillo, S. Nicolopoulos, D. Bultreys, S. Rouvimov, and P. Moeck, Automated nanocrystal orientation and phase mapping in the transmission electron microscope on the basis of precession electron diffraction, Z. Kristallogr. **225**, 103 (2010).

[33] C. Ophus, Four-dimensional scanning transmission electron microscopy (4D-STEM): From scanning nanodiffraction to ptychography and beyond, Microsc. Microanal. **25**, 563 (2019).

[34] I. MacLaren, T. A. Macgregor, C. S. Allen, and A. I. Kirkland, Detectors—The ongoing revolution in scanning transmission electron microscopy and why this important to material characterization, APL Mater. **8**, 110901 (2020).

[35] *Electron Microscopy of Thin Crystals*, edited by P. B. Hirsch, A. Howie, R. B. Nicholson, D. W. Pashley, and M. J. Whelan (Butterworths, London, 1965).

[36] B. H. Savitzky *et al.*, py4DSTEM: A software package for four-dimensional scanning transmission electron microscopy data analysis, Microsc. Microanal. **27**, 712 (2021).

[37] C. Ophus, S. E. Zeltmann, A. Bruefach, A. Rakowski, B. H. Savitzky, A. M. Minor, and M. C. Scott, Automated crystal orientation mapping in py4DSTEM using sparse correlation matching, Microsc. Microanal. **28**, 390 (2022).

[38] https://orix.readthedocs.io/en/stable/

[39] R. Bassiri, K. Evans, K. Borisenko, M. Fejer, J. Hough, I. MacLaren, I. Martin, R. Route, and S. Rowan, Correlations between the mechanical loss and atomic structure of amorphous TiO_2-doped Ta_2O_5 coatings, Acta Mater. **61**, 1070 (2013).

[40] G. Favaro *et al.*, Reduction of mechanical losses in ion-beam sputtered tantalum oxide thin films via partial crystallization, Classical Quantum Gravity **41**, 105009 (2024).

[41] Ã. Lalande, A. W. Lussier, C. Lévesque, M. Ward, B. Baloukas, L. Martinu, G. Vajente, G. Billingsley, A. Ananyeva, R. Bassiri, M. M. Fejer, and F. Schiettekatte, Zirconia-titania-doped tantala optical coatings for low mechanical loss Bragg mirrors, J. Vac. Sci. Technol. A **39**, 043416 (2021).

[42] D. Diksha, A. Amato, V. Spagnuolo, G. I. McGhee, M. Chicoine, C. Clark, S. Hill, J. Hough, R. Johnston, R. Keil, N. Mavridi, S. Reid, S. Rowan, T. Schapals, F. Schiettekatte, S. C. Tait, I. W. Martin, and J. Steinlechner, Optical properties of germania and titania at 1064 nm and at 1550 nm, Classical Quantum Gravity **41**, 125006 (2024).

[43] J. Steinlechner, I. W. Martin, R. Bassiri, A. Bell, M. M. Fejer, J. Hough, A. Markosyan, R. K. Route, S. Rowan, and Z. Tornasi, Optical absorption of ion-beam sputtered amorphous silicon coatings, Phys. Rev. D **93**, 062005 (2016).

[44] R. Schnabel, M. Britzger, F. Brueckner, O. Burmeister, K. Danzmann, J. Duck, T. Eberle, D. Friedrich, H. Luck, M. Mehmet, R. Nawrodt, S. Steinlechner, and B. Willke, Building blocks for future detectors: Silicon test masses and 1550 nm laser light, J. Phys. Conf. Ser. **228**, 012029 (2010).

[45] E. Hirose, D. Bajuk, G. Billingsley, T. Kajita, B. Kestner, N. Mio, M. Ohashi, B. Reichman, H. Yamamoto, and L. Zhang, Sapphire mirror for the KAGRA gravitational wave detector, Phys. Rev. D **89**, 062003 (2014).

[46] G. D. Cole, Cavity optomechanics with low-noise crystalline mirrors, in *Optical Trapping and Optical Micromanipulation IX*, edited by K. Dholakia and G. C. Spalding, Vol. 8458 of Society of Photo-Optical Instrumentation Engineers (SPIE) Conference Series (2012), p. 845807, 10.1117/12.931226.

[47] G. D. Cole, W. Zhang, M. J. Martin, J. Ye, and M. Aspelmeyer, Tenfold reduction of Brownian noise in high-reflectivity optical coatings, Nat. Photonics **7**, 644 (2013).

[48] J. Steinlechner, I. W. Martin, A. Bell, G. Cole, J. Hough, S. Penn, S. Rowan, and S. Steinlechner, Mapping the optical absorption of a substrate-transferred crystalline AlGaAs coating at 1.5 μm, Classical Quantum Gravity **32**, 105008 (2015).

[49] G. D. Cole, W. Zhang, B. J. Bjork, D. Follman, P. Heu, C. Deutsch, L. Sonderhouse, J. Robinson, C. Franz, A. Alexandrovski, M. Notcutt, O. H. Heckl, J. Ye, and M. Aspelmeyer, High-performance near- and mid-infrared crystalline coatings, Optica **3**, 647 (2016).

[50] A. Lin, R. Bassiri, K. Craig, A. Cumming, M. Fejer, J. Harris, K. Haughian, J. Hough, A. Markosyan, I. Martin, S. Reid, R. Route, and S. Rowan, Epitaxial integration of monocrystalline III–V coatings on silicon for thermal noise reduction, in *Optical Society of America, Optical Interference Coatings*, edited by M. Tilsch and D. Ristau, OSA Technical Digest, https://www.osapublishing.org/abstract.cfm?uri=OIC-2013-MA.2.

[51] A. C. Lin, R. Bassiri, S. Omar, A. S. Markosyan, B. Lantz, R. Route, R. L. Byer, J. S. Harris, and M. M. Fejer, Epitaxial growth of GaP/AlGaP mirrors on Si for low thermal noise optical coatings, Opt. Mater. Express **5**, 1890 (2015).

[52] A. V. Cumming, K. Craig, I. W. Martin, R. Bassiri, L. Cunningham, M. M. Fejer, J. S. Harris, K. Haughian, D. Heinert, B. Lantz, A. C. Lin, A. S. Markosyan, R. Nawrodt, R. Route, and S. Rowan, Measurement of the mechanical loss of prototype GaP/AlGaP crystalline coatings for future gravitational wave detectors, Classical Quantum Gravity **32**, 035002 (2015).

[53] P. G. Murray, I. W. Martin, K. Craig, J. Hough, S. Rowan, R. Bassiri, M. Fejer, J. Harris, B. Lantz, A. Lin, A. Markosyan, and R. Route, Cryogenic mechanical loss of a single-crystalline GaP coating layer for precision measurement applications, Phys. Rev. D **95**, 042004 (2017).

[54] G. Sosale, D. Almecija, K. Das, and S. Vengallatore, Mechanical spectroscopy of nanocrystalline aluminum films: Effects of frequency and grain size on internal friction, Nanotechnology **23**, 155701 (2012).

[55] G. Pezzotti, Internal friction of polycrystalline ceramic oxides, Phys. Rev. B **60**, 4018 (1999).

[56] G. I. McGhee *et al.*, Titania mixed with silica: A low thermal-noise coating material for gravitational-wave detectors, Phys. Rev. Lett. **131**, 171401 (2023).

[57] D. Diksha, A. Amato, V. Spagnuolo, G. McGhee, M. Chicoine, C. Clark, S. Hill, J. Hough, R. Johnston, R. Keil, N. Mavridi, S. Reid, S. Rowan, T. Schapals, F. Schiettekatte, S. Tait, and I. W. Martin, and J. Steinlechner, Optical properties of germania and titania at 1064 nm and at 1550 nm, Classical Quantum Gravity **41**, 125006 (2024).

[58] 10.5525/gla.researchdata.1866